مجله بلورشناسی و کانی شناسی ایران
انجمن بلورشناسی و کانی شناسی ایران
سال هفدهم، شمارهٔ ۴، زمستان ۸۸، از صفحهٔ ۷۱۶ تا ۷۳۳

سنگ‌شناسی و ژئوشیمی باتولیت قوشچی، شمال غرب ایران

مهران ادوای[1*]، احمد جهانگیری[1]، منصور مجتهدی[1]، جلیل قلمقاش[2]

۱- دانشگاه تبریز، دانشکده علوم، گروه زمین شناسی
۲- سازمان زمین شناسی و اکتشافات معدنی کشور

(دریافت مقاله: ۸۸/۱/۱۷ ، نسخه نهایی ۸۸/۵/۲۲)

چکیده: باتولیت قوشچی با مساحت تقریبی ۱۵۰ کیلومترمربع در شمال غرب ایران و زون سنندج- سیرجان واقع شده و به داخل سنگ‌های پرمین نفوذ کرده است. این تودهٔ نفوذی با سنگ‌های ته‌نشستی الیگو- میوسن (سازند قم) پوشیده شده است. باتولیت قوشچی شامل پنج تودهٔ مختلف است: الف) گابرو- دیوریت، ب) بیوتیت گرانیت، ج) فلدسپات گرانیت قلیایی، د) سینیت، ه) دایک‌های آپلیتی. گابرودیوریت ها قدیمی ترین واحد نفوذی در منطقه هستند که با واحد بیوتیت گرانیتی، زون تداخلی نشان می‌دهند. این واحد نفوذی ماهیت درون صفحه‌ای و تولئیتی دارد. گرانیت‌های قلیایی، بافت گرافیک، میکروگرانوفیری و پرتیتی دارند که نشانگر جایگیری در عمق کم و طبیعت هیپرسولووس آن‌هاست. از نظر ژئوشیمیایی این سنگ‌ها ویژگی‌های پتاسیم قلیایی بالا، متاآلومین تا کمی پرآلکالن دارند. گرانیت‌های قلیایی نسبت به بیوتیت گرانیت‌ها حاوی مقادیر پائین Sr، Rb ، Ba ، TiO_2 ، Fe_2O_3 ، CaO ، Al_2O_3 و دارای مقادیر بالای Zr، Y، Th ، Nb، K_2O ، Na_2O و SiO_2 هستند. گرانیت‌های قلیایی از نوع A، و درون صفحه‌ای بوده و احتمالاً با تبلور جدایشی نسبتاً بالای ماگماهای مافیک مشتق شده از گوشته حاصل شده‌اند. پلاژیوکلاز و آمفیبول دو فاز مهم حین تبلور جدایشی هستند. گرانیت‌های قلیایی از زیرگروه A_1 (مشتق شده از گوشته) محسوب می‌شوند که یک جایگاه غیرکوهزایی برای آن‌ها پیشنهاد می‌شود. بیوتیت گرانیت‌ها و سینیت‌ها پرآلومین بوده و خاستگاه پوسته‌ای دارند.

واژه‌های کلیدی: *گرانیت‌های نوع A، سنگ‌شناسی، ژئوشیمی، زون سنندج- سیرجان، باتولیت قوشچی.*

[*] نویسنده مسئول، تلفن: ۳۳۰۰۹۳۱ (۰۴۱۱) ۹۸+، نمابر: ۳۳۵۶۰۲۹ (۰۴۱۱) ۹۸+، پست الکترونیکی: mehran_advay@yahoo.com

Vol. 17, No. 4, Winter 1388/2010

Petrology and geochemistry of Ghoshchi batholith, NW Iran

Mehran Advay[1*], Ahmad Jahangiri[1], Mansour Mojtahedi[1], Jalil Ghalamghash[2]

Department of Geology, Faculty of Natural Sciences, University of Tabriz, Iran[1]
Research Institute of Earth Sciences, Geological Survey of Iran, Tehran, Iran[2]

(Received: 5/4/2009, in revised form: 12/8/2009)

Abstract: The Ghoshchi batholith, ~150 km^2 in size is a granitoidic pluton, which intruded the Permian country rocks, in Sanandaj-Sirjan Zone, NW Iran. This granitoidic pluton is covered by Oligocene-Miocene sedimentary rocks known as Qom Formation. The Ghoshchi batholith comprises five plutons with following compositions: (a) gabbro-diorite (b) biotite granite, (c) alkali granite, (d) syenites, and (e) aplitic dikes. Gabbro-diorites are the oldest intrusive unit and have interaction zone with biotite granites. These rocks have within-plate tholeiitic nature. Graphic, microgranophyric, and perthitic textures can be found in alkali-feldspar granites, indicate their shallow emplacement depth and hypersolvus nature. Alkali-feldspar granites geochemically are high-k alkaline, metaluminous to mildly peralkaline. The alkali-feldspar granitic rocks contain lower Al_2O_3, CaO, Fe_2O_3, TiO_2, Ba, Rb, and Sr but higher SiO_2, Na_2O, K_2O, Nb, Th, Y and Zr than biotite granites samples. Alkali-feldspar A-type within-plate granites were presumably formed by high degree of fractional crystallization of mantle derived mafic magmas. Plagioclase and amphibole are two main fractionated minerals. The Alkali-feldspar granites fall into the A_1 group (mantle derived) suggesting an anorogenic tectonic setting. Biotite granites and syenites are peraluminous and have crustal source.

Keywords: *A-type granites; Petrology; Geochemistry; Sanandaj-Sirjan Zone; Ghoshchi batholith.*

Introduction

The Zagros orogen extends from NW to SE Iran and is formed by collision of Afro-Arabian continent and the Central Iran microcontinent in Late Cretaceous to Tertiary [1-6]. The width of this belt is about 200 km that extended 1500 km along Zagros main thrust fault (Fig. 1). Paleozoic rocks are common in the southeast of the belt, but are rare in the other parts [7], where the rocks are mainly Mesozoic in age. There are many plutons in the northern part of Sanandaj-Sirjan Zone (SSZ), NW Iran. In the Golpaygan area, the Sanandaj-Sirjan Zone can be subdivided into two parts (Fig.1) : (1) The southern part (South SSZ), which consists of rocks deformed and metamorphosed in Middle to Late Triassic; (2) The northern part (North SSZ), deformed in the Late Cretaceous, contains many composite intrusions including Alvand, Boroujerd, Arak and Malayer plutons [8]. Most of them were formed by two main phases of mafic and felsic intrusions and belong to Mesozoic to Tertiary time (Table 1). In some plutons, primery mafic and felsic rocks were intruded by third phase of alkaline granites.

*Corresponding author, Tel.: +98 (0411) 3300931, Fax: +98 (0411) 3356029, Email: mehran_advay@yahoo.com

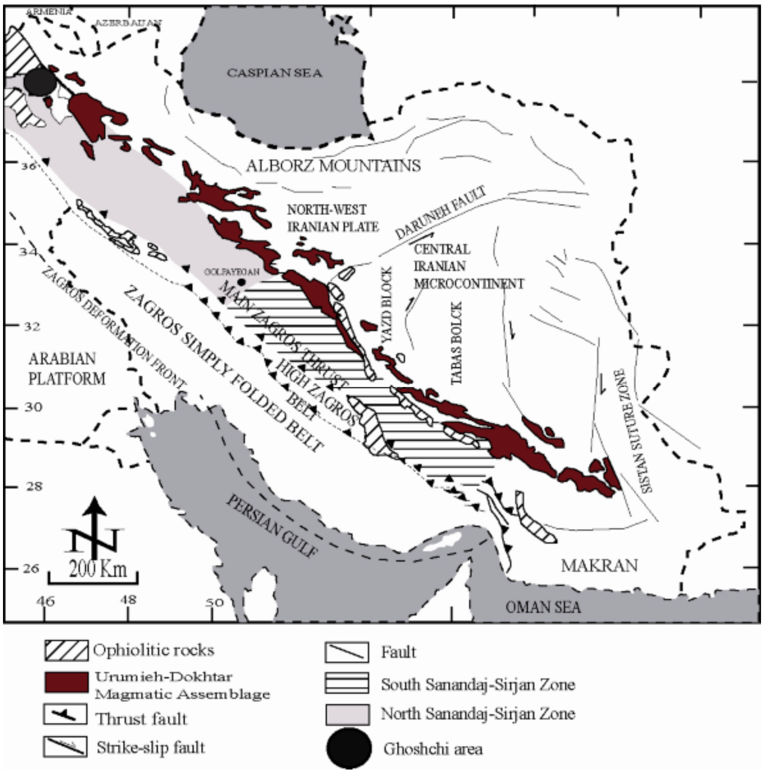

Fig. 1. Main tectonic units of Iran (Extracting from [47]). Studied area shown by a circle.

Table 1. Some plutonic rocks in northern Sanandaj-Sirjan Zone

Pluton Name	Number of phase & Rock composition	Age	Source	Tectonic setting	References
Almoghulagh	Quartz syenite-granite & gabbro diorite	144 ±17 Ma	S-type	Subduction related	[13], [14] & [55]
Astane-ye Arak	Andalosite bearing granodiorite	98.9 ± 1.5 Ma	S-type	-	[56], [13]
Boroujerd-Malayer	Three phases with composition of: quartz diorite, granite, granodiorite, aplite & pegmatite	Late Jurassic-Paleocene, 3 phases with age: 1- 117-120Ma 2- 99 Ma 3- 52-70 Ma	Different sources, S-type granites	One phase has been reported CAG type	[57], [58], [59]
Aligudarz-Miyandasht	Six plutons and minimum 3 phase include: gabbro diorite, doleritic dykes & granite	Post-Cretaceous and Pre-Eocene	Basic rocks from partial melting of mantle and acidic rocks from partial melting of continental crust	POG type	[59], [60], [61]
Alvand	Five phases include: 1- gabbro diorite 2- tonalite 3,4- porphyric granite 5- hololeucocrate granite	Late Cretaceous-Paleocene 64-70 Ma	Include: I , S and other different-type granites	CAG type	[62], [63]
Pichaghchi	Granite, granodiorite & tonalite	72-76 Ma	I and H-type	CAG type	[64]

Obviously, in many composite plutons, mafic rocks have been generated before felsic ones. Obvious differences in rock composition indicate different sources involved in petrogenesis of each rock group [9-12]. These studies show that there are I-, S-, H-, and in a small volume A-type granites in this zone. In these studies, the source of basic to intermediate rocks and I-type granites is attributed to partial melting of mantle (primary or evolved) or underlying crust, and the source of acidic rocks (S- and A-type granites) is attributed to partial melting of continental crust (Table 1).

Many researchers [10-14] believe that Golpaygan-Urumieh plutons are generated due to subduction related magmatism and they have reported these rocks similar to active continental margin granites. In some other studies, plutonic rocks, is attributed to extentional regimes [15] (Table 1). Ghoshchi pluton is a northwestern portion of Golpaygan-Urumieh intrusions that crops out in north of Urumieh city. Similar to the other plutons, the Ghoshchi batholith includes both mafic and felsic parts, which seems that emplaced at Post-Cretaceous to Pre-Miocene time [15-16]. Alkali granite of Ghoshchi formed main volume of batholith which reported as A-type granite by [9] and metasomatism product of mafic rocks by [16].

In this paper, we present new information about geology, petrography and geochemistry of Ghoshchi pluton. Also, we will discuss the relationship between mafic and felsic intrusions and finally we present a tectonomagmatic setting model for studied granites.

Geological setting

The Ghoshchi batholith is located in the northern part of Sanandaj-Sirjan Zone, NW Iran (Fig.1). The basement rocks of Ghoshchi area is metamorphic rocks with amphibolite and green schist facies attested to Late-Precamberian.

Gneiss, metarhyolite, and schists are the oldest rocks. The metamorphic rocks are overlaid by Permian to Jurassic sedimentary rocks. The metamorphic rocks are intruded by plutonic rocks.

Ghoshchi batholith comprises five distinct intrusive rocks including 1) gabbro-diorite, 2) biotite granite (BG), 3) alkali-feldspar granite, 4) Syenite, and 5) Aplitic to diabasic dikes.

The gabbro-diorites crop out in northern part of the batholith in the metamorphic host rocks (Fig. 2). These mafic rocks were intruded by younger granitic members and dibasic dikes. They are enclave-free. Gabbro-dioritic rocks of Ghoshchi are undeformed, fresh and with minor alteration.

Biotite granites occupy about 5-10% of the total area of batholith. Biotite granitic rocks are intruded by alkali-feldspar granite veins and dikes. They have metasedimentry and mafic enclaves. Biotite granites in contact with mafic member of batholith contain lots of mafic enclaves. In some places, e.g. along the old road of Salmas to Ghoshchi, mingling-mixing features of gabbro-diorite and biotite granite magmas can be observed (Fig. 3a). Magmatic interaction is characterized by mafic pillow-like masses, milimeteric to meteric in size, in a grey-coloured granitic host rocks. The contact between the dioritic pillows and the surrounding and net-veining granite are often sharp or locally diffuse. Such features have been regarded as evidence of the coexistence of mafic and felsic magmas [10].

Main host rocks of Goshchi alkali-feldspar granites are Permian sedimentary rocks including conglomerate and limestone which are covered by Oligocene-Miocene limestones. Alkali-feldspargranites occupy about 50-60% of total outcrop of batholith about 75 to 90 square kilometer area and varies from hololeucocratic to leucocratic rocks and pink to light gray in color. This unit has miarolitic cavities indicating its shallow depth emplacement. The alkali-feldspar granite has no enclaves. Contact of alkali-feldspar granites with gabbro-diorites and biotite granites is sharp.

Syenitic group occupies about 5% of the total outcrop area. This unit is very small as apophyse that cut the biotite granites (Fig. 3b). Thickness of this unit is 2 meter.

There are some aplitic and pegmatitic dikes that cut mafic rocks. Furthermore, some quartz-feldspatic veins cut the mafic and felsic rocks in the studied area. Thickness of veins in this unit is lower than 10 cm.

Based on stratigraphical studies, Ghoshchi batholith is Post-Permian and Pre-Miocene, however [17] have attributed this pluton to Early Paleogene.

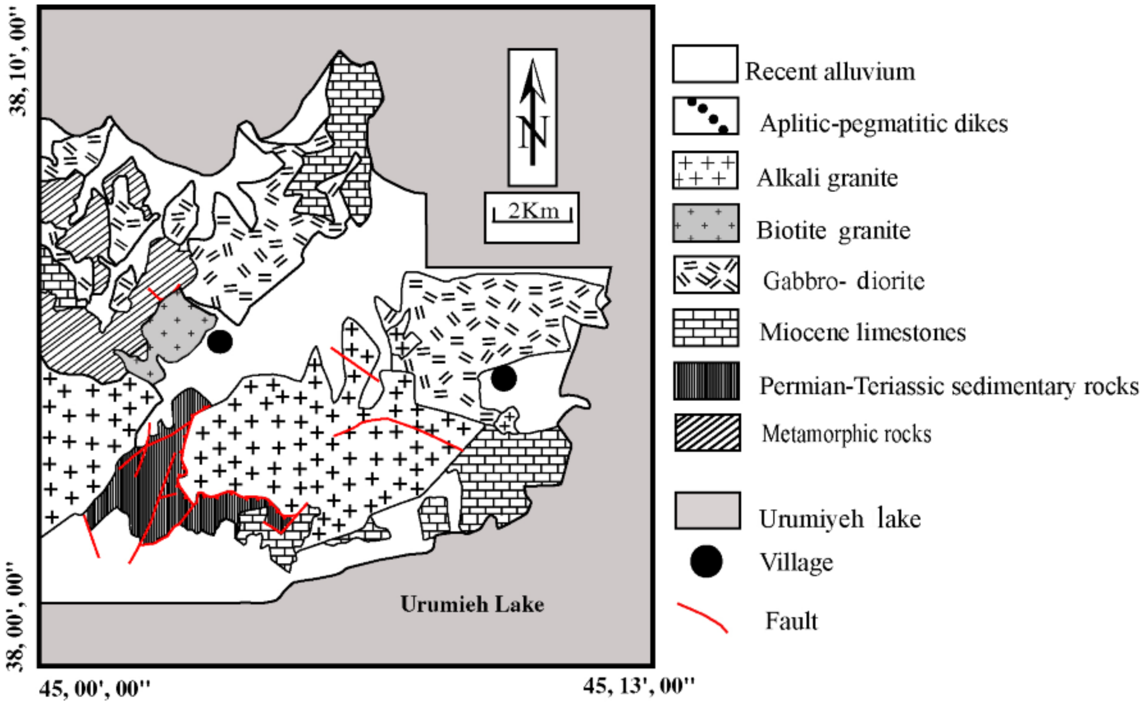

Fig. 2. schematic geological map of the Goushchi area

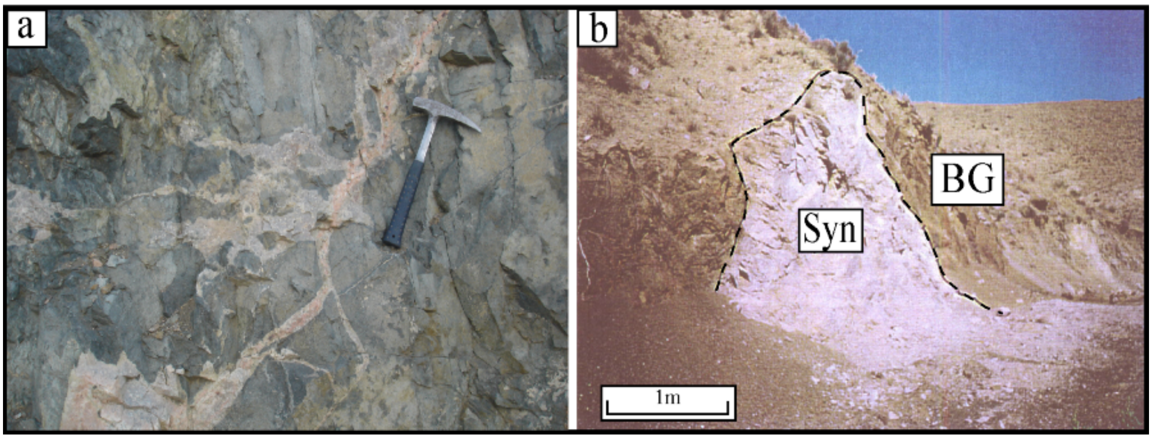

Fig. 3. a) Interaction (mingeled) zone between gabbro-diorites and biotite granites, b) Syenites cut the biotite granites.

Petrography

Gabbro-diorites

Modal compositions of the representative plutonic rocks are plotted in Figure 5a and representative mineral compositions are given in Table 2.
The Gabbro-dioritic rocks of Ghoshchi batholith is mainly made of olivine gabbro, gabbro, norite, diorite and quartz diorite.

Gabbro-dioritic rocks are dark grey in colour. Euhedral plagioclase (andesine to bytownite), clinopyroxene (augite), olivine, orthopyroxene (hypersthene), hornblende and biotite are the main minerals of the rock. Locally, quartz is present. Euhedral apatite, titanite, opaques and zircon form accessory minerals. Average grain size is about 1-4mm.

Table 2- Modal composition of selected samples from Ghoshchi batholith.

Rock type	Gabbro-diorite		Biotite granite				Alkali-feldspar granite			Syenitic rocks			
Sample ID	**GD1**	**GD2**	**BG1**	**BG2**	**BG3**	**BG4**	**AG1**	**AG2**	**AG3**	**S1**	**S2**	**S3**	**S4**
Quartz	0.6	1.9	25	23	22.5	22	25.4	22.5	26.6	2.5	3	3	2.9
Plagioclase	70	69	17.3	19	17.9	30	6	3	4.6	15.6	10	18	6.4
K-feldspar	0.4	0.5	42	40	44	33	59	66	61	66	67	58	71
Amphibole										4.3	4.2	4.5	3.4
Biotite	2.5	3.7	14.5	16.5	14	11.5	3.1	3.3	2.5	5.7	9	8.1	8
Clinopyroxene	15.8	16								3	2	2	4
Orthopyroxene	4.2	4.1											
Opaque	5	4.2	0.5	0.7	1.2	2	5	3.4	2.3	2.8	4.8	6.2	4.2
Titanite	0.1	< 0.1					0.6	1	1.9				
Apatite	1.3	0.5	0.1	0.1	0.1					0.1		0.1	
Zircone	0.1	0.1	0.1		0.1		0.1	0.1	0.1			0.1	0.1
Epidote			0.3	0.5	0.9	1							
Chlorite			0.2	0.2	0.3	0.5	0.8	0.7	1				

Biotite granites

The Biotite granites straddle the fields of monzo- to syenogranites in Figure 5a. All these granites are gray in colour; displaying a medium-grained size and an equigranular texture.

This unit consists essentially of quartz, alkali feldspar, plagioclase, biotite, and muscovite (Fig. 4c). Quartz is anhedral and generally has undulose extinction. Biotite is anhedral to subhedral with green to brown colour. Locally, biotite has been altered to muscovite as a result of to leave the Mg, Fe, and Ti (Fig. 4d). Zircon and apatite are accessory minerals. Chlorite and epidote are alteration products.

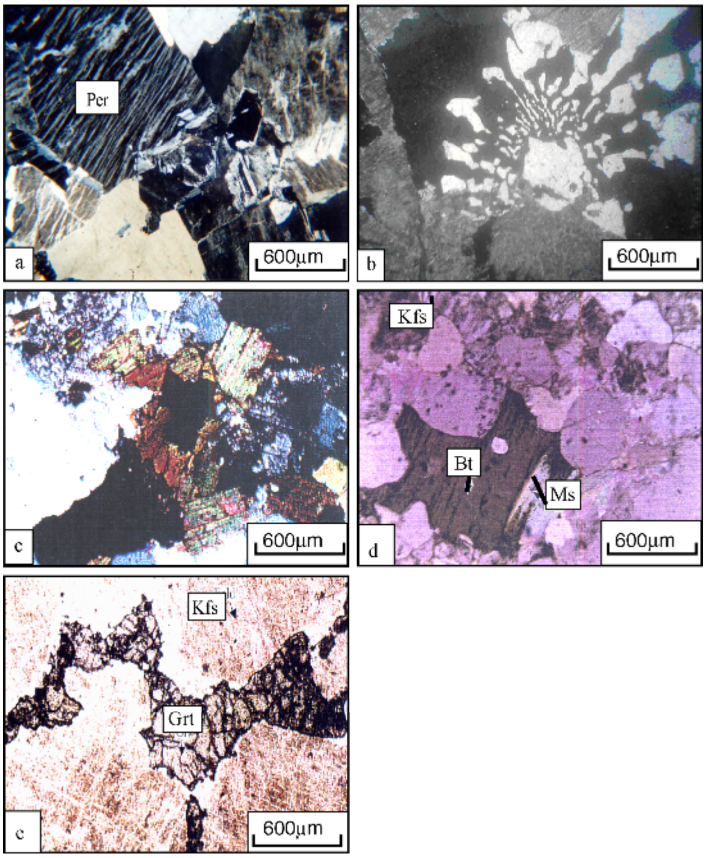

Fig. 4. Photos from petrographical features in felsic rocks. a) microperthitic and granular textures in alkali-feldspar granites. Crossed Nicols, b) Granophyric texture, Crossed Nicols, c) Granular texture in biotite granites. Crossed Nicolss, d) Biotite has been altered to muscovite. Crossed Nicols, e) Generation of Garnet among alkali feldspars in syenitic rocks. Plane Polarised Nicols, Kfs= K-feldspar, Bt= Biotite, Ms= Muscovite, Grt= Garnet, Per = Perthite.

Alkali-feldspar granites

These rocks straddles the field of alkali feldspar granite in Figure 5a. The obvious textures in this unit are granular, microperthitic, porphyric, and micrographic to granophyric (Figs. 4a, b). Subhedral to euhedral grains of quartz, perthitic K-feldspar, plagioclase, and biotite make up alkal-feldspar granites. Locally amphibole (arfvedsonite-riebeckite), about 5%, exists. The perthitic nature of the K-feldspar in this unit indicates their vapor absent condition of crystallization. Alkali feldspar minerals are anhedral including orthoclase and microcline with microgranophyric to graphic textures.

Brown to green Biotite is replaced by chlorite along cleavage planes, locally. Zircon and titanite are common accessory minerals occurring as euhedral to subhedral magmatic crystals in the matrix. Biotites has pleochroic halos around zircon inclusions.

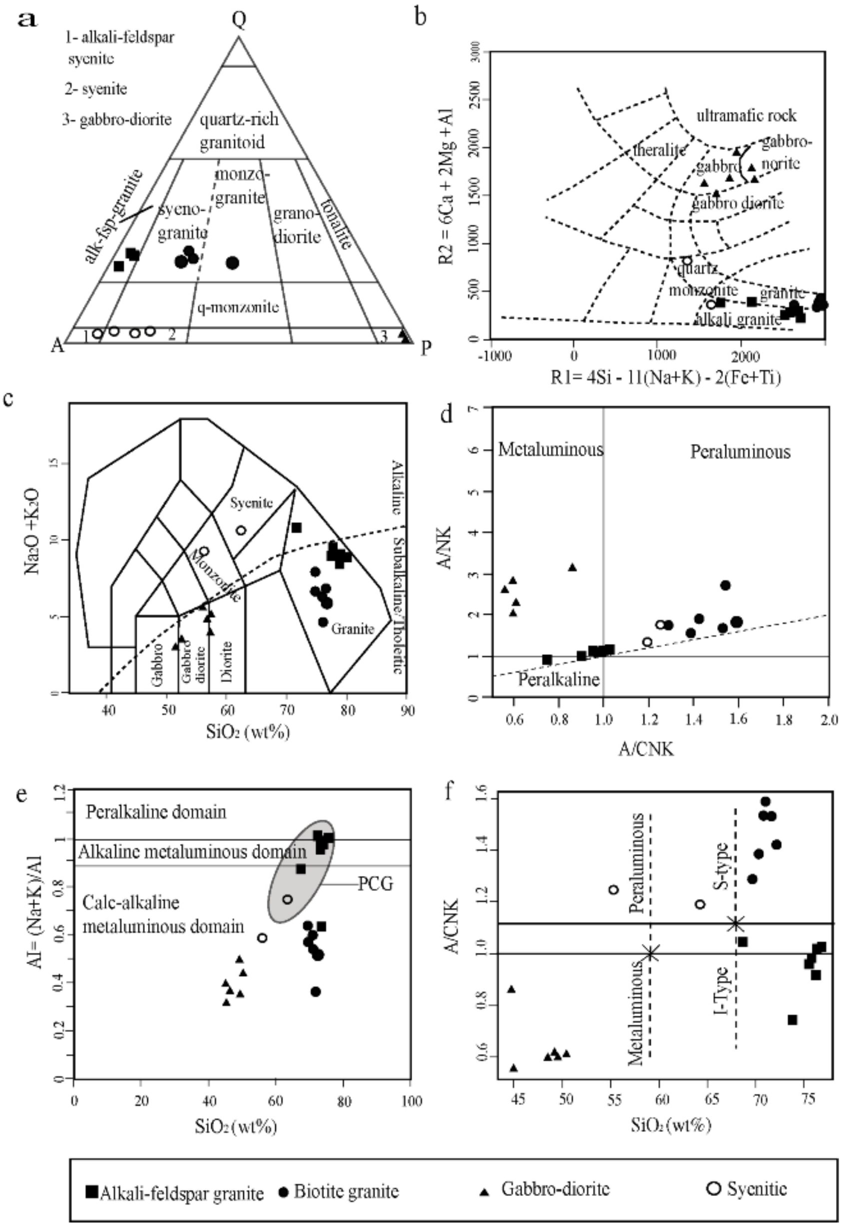

Fig. 5. Modal and chemical classification diagrams. (a) Modal classification of igneous rocks from [50] (b) R1-R2 cationic classification of [19]. (c) Na_2O+K_2O vs. SiO_2 from [20]. (d) Al/ (Na+K) vs. Al/ (Ca+Na+K) (mol. %): field boundaries are from [51]. (e) Agpaitic index (AI) vs. SiO_2 diagram [52]. The post-collision granite (PCG) field is from [22]. (f) SiO2 vs. A/CNK diagram. Peraluminous and metaluminous fildes are after [53] and I-type and S-type fields are after [54].

Syenites

The syenites plot in the fields of alkali feldspar syenite and syenite in Figure 5a. The rocks have granular texture with fine to medium grain size and consists essentially of perthitic alkali feldspar, plagioclase, garnet, clinopyroxene, quartz, riebeckite, biotite, sphene, and opaque minerals.

Alkali feldspar as anhedral to subhedral minerals forms the main volume of the rock. Orthoclase, with carlsbad twin and microperthite with striped pattern are two different kinds of alkali feldspar. After alkali feldspar, plagioclase is the main mineral in syenites.

Garnet is the product of late stage of crystallization in syenitic rocks and it fills spaces between alkali feldspars (Fig. 4e).

Fe-rich biotites together with riebeckite have been formed in spaces between alkali feldspars. Allanite is accessory mineral in these rocks.

Aplitic and diabasic dikes

Plagioclase (andesine), amphibole (hornblende), biotite, and chlorite are main minerals in the diabasic dikes. Opaque minerals and very small titanite are accessory minerals.

Many aplitic dikes intruded Ghoshchi batholith. They are hololeucocratic with white colour and equi-granular texture. This rock is consisted of quartz, alkali feldspar, plagioclase, biotite and chlorite. Frequently, quartz is anhedral and has fine to medium grain size. Alkali feldspar is anhedral and includes orthoclase and microcline. Plagioclase is subhedral and it has polysynthetic twining.

Geochemistry

Analytical method

In order to study the geochemistry of the Ghoshchi batholith, 21 representative rock samples with minimal alteration were chosen for chemical analysis. Selected whole rock samples were analyzed for major elements using XRF at GSI (Geological Survey of Iran) laboratory. Samples were analysed for trace and rare earth elements by ICP-Mass Spectrometry at ALS CHEMEX Ltd, Canada. The results of the XRF and ICP-MS analyses are presented in Table 3.

Table 3. Major and trace elements of felsic and mafic rocks in Ghoshchi area.

	Alkali Granites							**Biotite Granites**						**Syenites**		**Gabbro-Diorites**					
	Major Oxides, wt%																				
SiO_2	69	74	75	75	77	77	76.1	71	70.3	70	72	71	72	55.3	64.1	50	45	49	49	44.7	49
TiO_2	0.2	0	0.2	0.2	0.2	0.2	0.19	0.4	0.24	0.4	0.4	0.2	0.4	1.35	0.18	1.6	2	2	2.6	0.9	2.2
Al_2O_3	15	11	11	12	12	11	11.3	14	14.7	13	14	14	15	17.4	15.8	15	12	16	14	11.8	14
Fe_2O_3*	1.6	1.5	2.4	2.1	1.8	2.1	1.98	4.4	2.42	3	2.8	2.4	4.4	5.21	1.6	8.2	12	9.9	12	13.2	13
MnO	0	0	0.1	0.1	0.1	0.1	0.09	0	0.02	0	0	0	0	0.04	0.02	0.2	0.2	0.2	0.2	0.17	0.2
MgO	0.3	0.4	0.1	0.1	0.1	0.1	0.09	0.5	0.29	0.5	0.4	2.3	0.4	5.17	0.26	5.7	15	5.3	6	19.9	6.2
CaO	0.7	1.4	0.5	0.4	0.1	0.1	0.49	0.4	0.61	1.5	1.4	0.6	2.4	2.05	0.63	10	9.1	9.9	8.8	5.45	10
Na_2O	2.9	4.4	3.3	3.8	3.2	3.5	3.76	2.8	2.58	2.3	2.2	1.6	1.3	2.48	2.81	3.5	2.5	4.3	3.8	1.86	2.5
K_2O	7.4	5.3	5	4.9	5.4	5	4.89	3.6	4.82	3.6	3.4	4.7	3.1	5.71	6.94	0.9	0.5	0.6	0.6	0.67	0.8
P_2O_5	0.1	0	0.1	0.1	0.1	0.1	0.09	0.2	0.02	0.1	0.1	0	0.1	0.23	0.09	0.2	0.3	0.4	0.5	0.13	0.4
	trace elements, ppm																				
Rb	203	196	168	173	174	182	177	146	261	267	176	175	191	81.7	83	19	15	12	11	17.3	10
Sr	20	8.3	16	16	12	11	16.3	73	329	390	518	527	453	162	171	238	341	311	287	105	282
Ba	150	37	106	115	69	132	143	804	777	767	818	804	822	1575	1535	267	193	439	550	86.4	238
Zr	206	565	514	438	407	506	410	187	155	134	134	142	160	769	777	160	107	163	226	101	154
Y	40	83	77	69	68	77	73.7	9	11.2	14	10	7.3	15	29.2	25	14	6	18	27	13.7	42
Nb	32	76	72	68	45	68	61.8	7.8	14	12	13	14	13	30.6	25	28	16	23	38	6.1	27
V	<5	<5	<5	<5	5	<5	<5	18	12	11	15	16	12	38	33	225	219	277	252	88	221
Cr	10	<10	10	10	10	10	10	20	35.2	39	42	39	45	20	20.4	244	810	83	147	2250	280
Co	91	48	49	82	66	71	67.8	46	22.7	20	19	14	11	27.2	25.7	35	89	40	45	113	47
Ni	<5	<5	<5	<5	<5	<5	<5	<5	29.7	23	21	29	19	<5	44.4	67	450	49	50	1110	64
Cu	<5	<5	<5	<5	<5	6	8	<5	<5	<5	<5	<5	<5	<5	<5	N.A.	N.A.	N.A.	N.A.	151	38

Table 3. (Continued)

Zn	29	141	74	51	42	53	65	26	25	18	15	19	30	76	68	100	99	111	132	98	147
Ga	20	30	28	27	28	28	30.3	17	13	15	12	10	13	25.7	11	N.A.	N.A.	N.A.	N.A.	10.7	19
Cs	3.6	1.8	0.9	0.7	2.3	1.1	2.49	2	2	2	2.2	2.1	2	1.34	1.43	N.A.	N.A.	N.A.	N.A.	0.6	0.3
La	90	68	87	82	55	96	81.5	30	43	37	29	27	33	40.5	33	33	16	8	15	8.5	24
Ce	168	123	170	150	103	96	158	62	66	74	56	54	59	70.5	68	17	60	16	65	17.8	53
Pr	18	16	19	18	14	23	19.1	7.3	8.2	9.1	8.8	7.4	7.1	7.97	7.66	N.A.	N.A.	N.A.	N.A.	2.21	7.2
Nd	59	63	71	65	54	88	71.9	28	26	22	29	30	31	31.4	30.2	N.A.	N.A.	N.A.	N.A.	9.5	32
Sm	10	14	15	14	12	19	15.4	6.4	7.3	5.9	8	7.7	6.2	6.3	6.9	N.A.	N.A.	N.A.	N.A.	2.34	8.3
Eu	0.5	0.7	0.6	0.6	0.7	0.8	0.86	0.7	0.77	0.7	0.7	0.8	0.7	2.08	2.01	N.A.	N.A.	N.A.	N.A.	0.71	2.4
Gd	9.9	15	16	14	13	19	15.8	6.6	6.1	7.3	8.1	6.8	8.4	6.48	6.7	N.A.	N.A.	N.A.	N.A.	2.56	9.2
Tb	1.5	2.6	2.5	2.3	2.2	2.8	2.52	1.1	1.21	1.1	1.3	1.4	1.1	0.95	0.98	N.A.	N.A.	N.A.	N.A.	0.43	1.5
Dy	8.1	16	14	14	13	16	14.6	7.1	6.2	5.8	7	7.8	7.4	5.46	5.14	N.A.	N.A.	N.A.	N.A.	2.63	9
Ho	1.6	3.3	2.8	2.8	2.6	3	2.89	1.4	1.3	1.5	1.6	1.2	1.2	1.13	1.19	N.A.	N.A.	N.A.	N.A.	0.55	1.8
Er	4.7	9.7	8.3	8.4	7.5	8.9	8.36	4.3	4.44	4.2	4.1	4.4	4.2	3.32	3.1	N.A.	N.A.	N.A.	N.A.	1.56	4.9
Tm	0.7	1.4	1.2	1.2	1	1.3	1.18	0.6	0.56	0.6	0.7	0.6	0.6	0.49	0.44	N.A.	N.A.	N.A.	N.A.	0.21	0.6
Yb	4.6	9.4	7.7	7.8	6.4	8.6	7.31	3.9	3.99	4	4	3.9	3.7	3.2	3.01	1.4	1.5	1.4	1.3	1.48	4.2
Lu	0.6	1.3	1.1	1.1	0.9	1.2	1.04	0.5	0.52	0.6	0.6	0.6	0.6	0.47	0.44	N.A.	N.A.	N.A.	N.A.	0.19	0.6
Hf	7	18	16	14	12	16	13.6	5.8	3.64	4.1	3.7	3.8	4.2	18.6	1.5	11	7	4	8	2.7	4.2
Ta	2.6	5.2	5.3	4.7	3.1	5.1	4.2	0.7	1.45	1.3	1.2	1.4	1.5	1.6	7.9	0.5	0.5	0.4	0.5	0.4	1.5
Th	36	24	33	27	14	24	21.1	16	16	14	13	12	15	3.76	3.3	2	2	0	0	2.13	1.3
U	4.4	6	9.5	4.8	2.8	4.8	3.65	2	2.01	3	2.1	2	1.9	1.49	1.33	1	2	0	0	0.52	0.3
Pb	16	15	17	26	8	14	27	21	22	18	16	22	19	14	12	2	6	7	14	<5	6

N.A. = Not Analysed

Rock classification

Using the cationic classsification [19] (Fig. 5b), mafic samples plot in gabbro and gabbro-norite fields. A few straddle the boundry between the gabbro and gabbro-diorite fields. The alkali granitic rocks occupy the alkali granite field, whereas the syenites and biotite granitic rocks fall mainly in the syenite to monzonite and granite fields respectively.

On the total alkali silica (TAS) diagram (Fig. 5c), as defined by [20] the Ghoshchi felsic rocks plot in the granite and syenite fields and Ghoshchi mafic rocks fall into the gabbroic diorite field. According to the K_2O vs. SiO_2 diagram of [21] Ghoshchi felsic rocks display medium-K to high-K characters (Fig. 7), while the Ghoshchi mafic rocks plot in the low-K field. On the other hand, Ghoshchi mafic rocks have alumina saturation indices (ASI), defined as the molar A/CNK= Al_2O_3/ (CaO+Na_2O+K_2O), of less than 1.1, indicating their metaluminous character, whereas, Ghoshchi felsic rocks have two distinct characters: alkali-feldspar granites are mainly metaluminous (except for one sample which shows peralkaline character) and, biotite granites and syenites are peraluminous (Fig. 5d). The agpaitic index (AI) of the felsic to mafic rocks of Ghoshchi complex, calculated as molar (Na+K)/Al, suggesting an alkaline metaluminous character for alkali-feldspar granitic rocks (Fig. 5e). In this diagram, the alkali granites occupy the field given by [22] for the Pan-African post-collision granites.

Biotite granites and syenites have peraluminous and S-type characteristics (Fig. 5f).

The alkali-feldspar granitic rocks exhibit anhydrous and hypersolvus characteristic of A-type magmas. In a series of diagrams designed by [23] to discriminate A-type granites (Figs. 6a-d) the alkali-feldspar granitic rocks plot in the A-type granite or close to the boundary of the A-type granite field, typical of metaluminous A-type granites [24] Whereas, the biotite granites and syenites plot in the field of I-, S- and M-type granitoids.

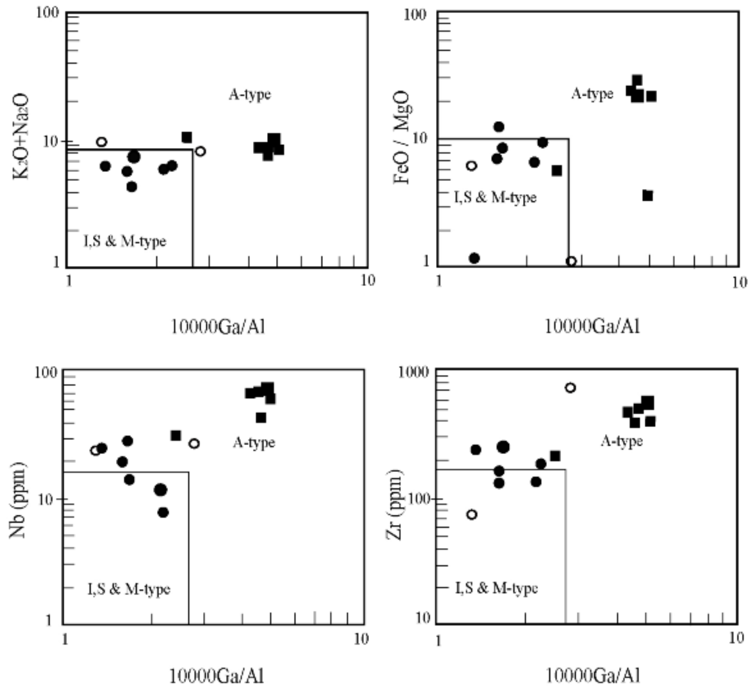

Fig. 6. $K_2O + Na_2O$, Nb, and Zr vs. 10000Ga/Al discrimination diagrams of [23]. Symbols as in Fig. 5.

Elements and oxide variations

Major and trace element variations were evaluated using selected Harker variation diagrams (Figs. 7 and 8). Compared to the biotite granites, alkali granites are characterized by rather high abundances of SiO_2, K_2O, Na_2O, Nb, Th, Y, Mn, and Zr with lower abundances of Al_2O_3, CaO, Fe_2O_3, TiO_2, Ba, Rb, and Sr (Fig. 8). The MnO abundances of alkali-feldspar granitic rocks are about 2-3 times lower than the average A-type granites (0.06%, see [23]). The gabbro-dioritic rocks have low abundances of K_2O, Rb, Y, and Zr. Na_2O content of these rocks is ranging from 1.86 to 4.26 (Fig. 7). The major and trace element compositions of the biotite granites tend to cluster or spread more or less vertically parallel to y-axis of the diagrams, partly as a function of the small range of silica values.

In the REE diagrams (Figs. 9a, b) each rock type show different patterns. The data are normalized to chondrite [25] and invariably show relative enrichment of light rare earth elements (LREE). Alkali-feldspar granites and biotite granites show clear negative Eu anomaly and gabbro-diorites show small negative anomaly, whereas syenites do not show this characters.

ORG-normalized spider diagrams [26] for alkali-feldspar granites and biotite granites indicate increasing trend from Yb to Rb. For alkalifeldspar granites Ba has intense negative anomaly and Rb and Th are considerably enriched compare to Nb and Ta. Ce, and Sm are enriched compared to adjacent elements (Fig. 9c). These selected enrichment (Ce and Sm), can be attributed to crustal interference or contamination. For biotite granites, Ba shows negative anomaly and Ce and Sm show positive anomalies.

In the (ocean ridge granite) ORG-normalized diagram (Fig. 9c), the alkali-feldspar granites are significantly enriched in Rb and Th relative to Nb and Ta and Ce and Sm are enriched relative to their adjacent elements on the diagram.

Primitive Mantle-normalized spider diagrams [27] for the investigated plutonic rocks (Fig. 9d) show enrichment in large ion lithophile elements (LILE) relative to high field strength elements (HFSE). The alkali-feldspar granites show Sr, Ba, Nb, and intense Ti negative anomalies, which are typical of subduction related magmas [26]. Gabbro-diorites have convex pattern in Primitive Mantle-Normalized diagram (Fig. 9d), as it has maximum content of Pb. The biotite granites show negative anomalies for Nb, La, and P and positive anomaly for Pb (Fig. 9e). Also, the syenitic rocks have positive anomalies in Rb, K, PB, and Zr (Fig. 9d).

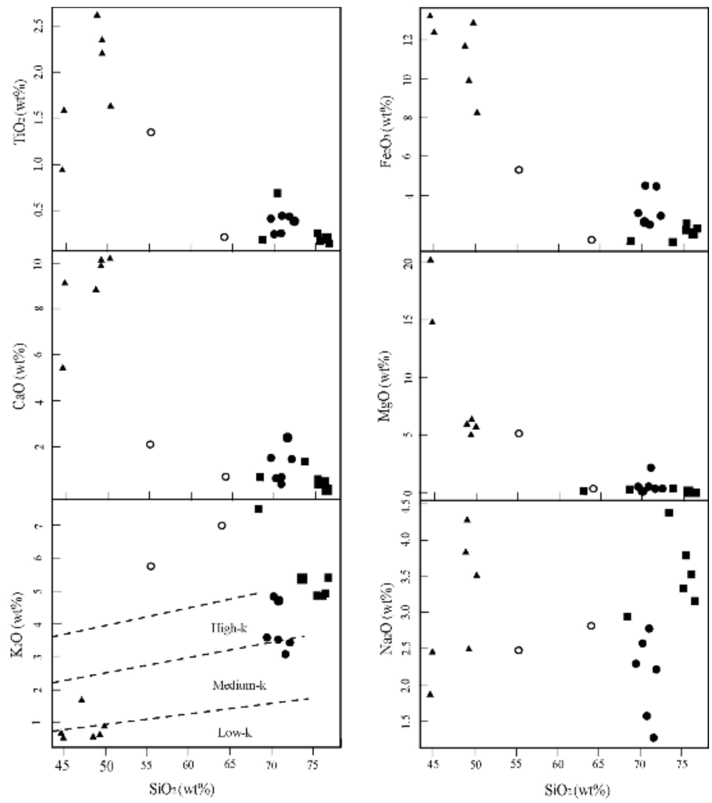

Fig. 7. Harker variation diagrams of selected major element oxides. Fields in K_2O vs. SiO_2 after [21] Symbols as in Fig. 5.

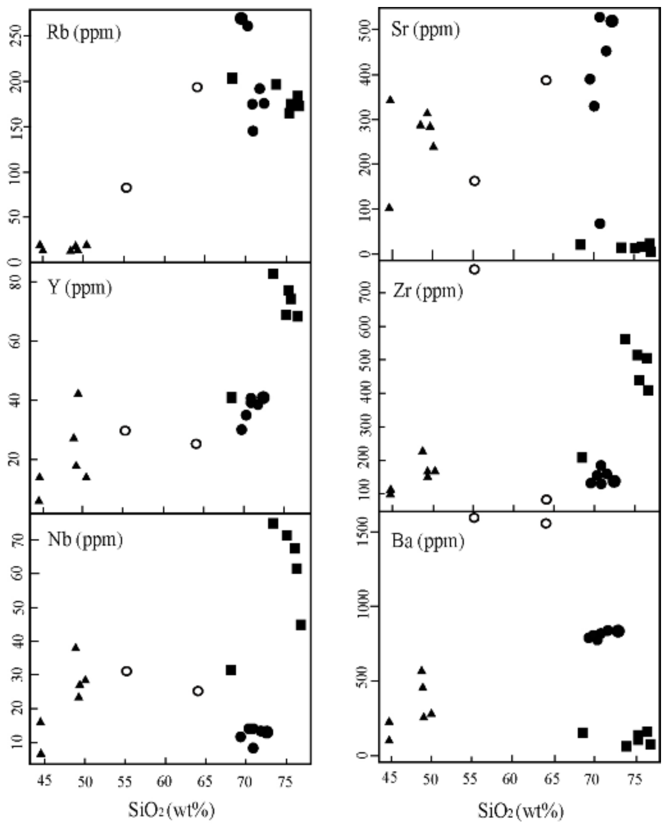

Fig. 8. Harker variation diagrams of selected trace elements. Symbols as in Fig. 5.

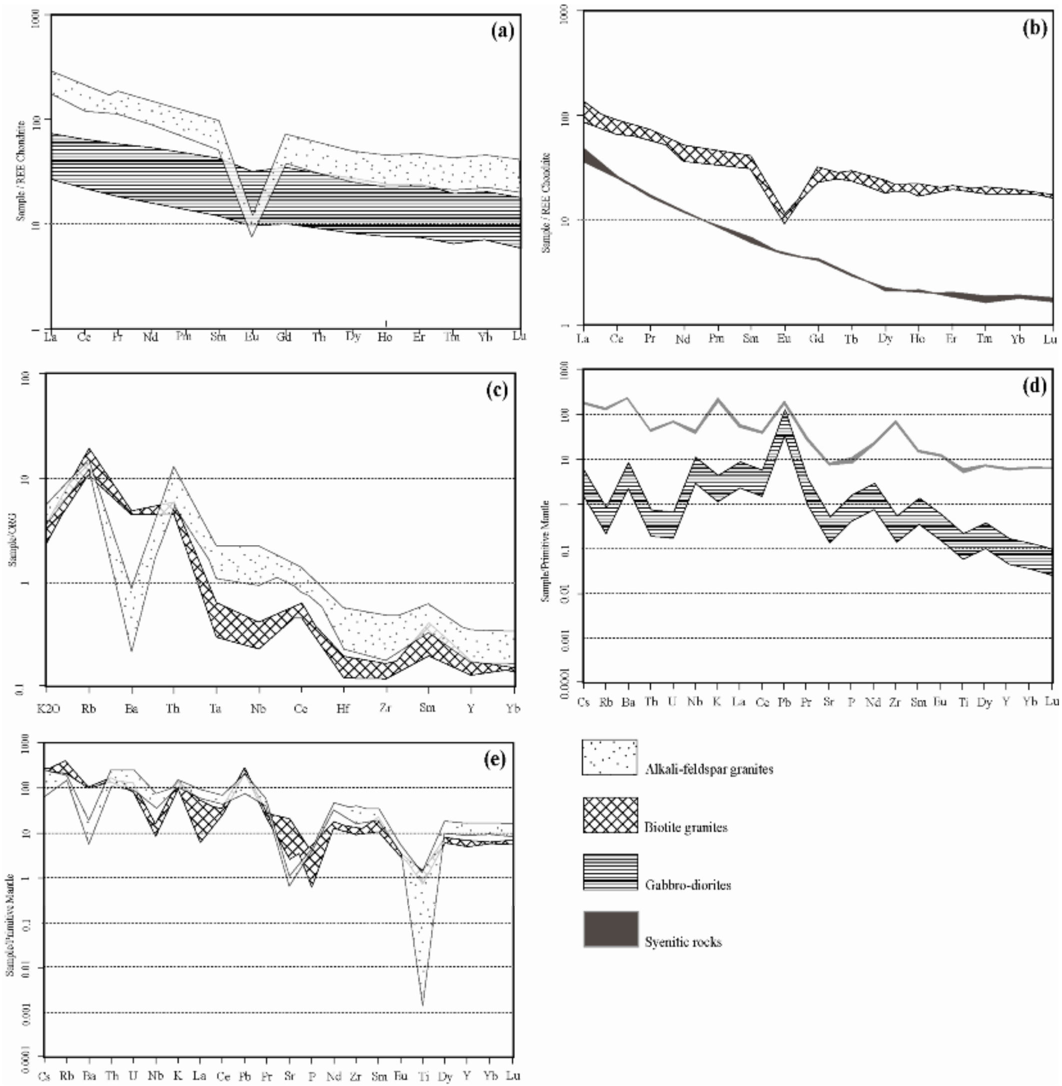

Fig. 9. REE and Spider diagrams for studied plutonic rocks. (a) REE diagram for alkali-feldspar granites and gabbro-diorites (b) REE diagram for biotite granites and Syenitic rocks (in a and b normalization values are from [25]. (c) ORG normalized spider diagram for alkali-feldspar granites and biotite granites (normalization values are from [26]). (d) Primitive Mantle normalized spider diagram for gabbro-diorites and Syenitic rocks. (e) Primitive Mantle normalized spider diagram for biotite granites and alkali-feldspar granites (in d and e normalization values are from [28]).

Discussion and conclusions

Tectonic setting

Using the tectonic discrimination diagrams of [26], the alkali-feldspar granites (Fig. 10) have characteristics of intra plate (WPG) and post-collision. Post-collision character of alkali-feldspar granites is confirmed by AI vs. SiO_2 diagram (Fig. 5d). Nevertheless, biotite granites have mainly VAG or syn-collision characteristics (I-type). Syenitic rocks show intra plate and VAG characteristics.

Gabbro-diorites show a tholeiitic trend using the classification diagrams of [28-29], also these rocks show continental basalts and within-plate character (Figs. 11c and d) using the classification diagrams of [30-31].

A-type granites can be formed in both post-orogenic and anorogenic settings [23-32]. [32] subdivided the A-type granites into A_1 and A_2 groups. The A_1 group is mantle-derived and are emplaced in an anorogenic setting such as continental rifts or other intraplate environments. The A_2 group comprises crustal derived magmas of a post-orogenic setting. Using the Rb/Nb vs. Y/Nb (Fig. 12) and Y-Nb-3×Ga (not shown) discrimination diagrams of [32] the alkali-feldspar granites fall into the A_1 group (except one sample) suggesting an anorogenic tectonic setting. Some samples of alkali-feldspar granites fall in boundary of A_1 and A_2 or in A_2 field.

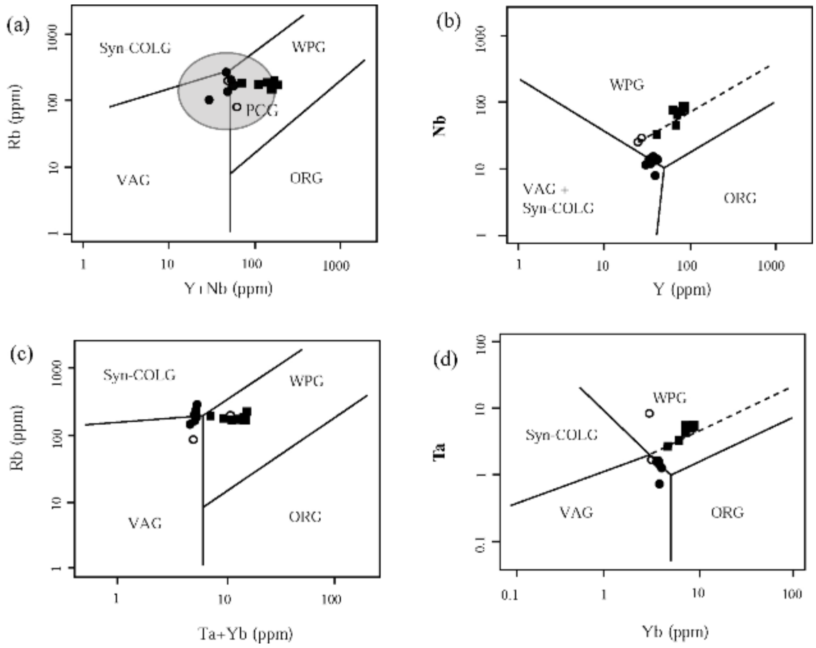

Fig. 10. Tectonic discrimination diagrams. (a) Rb vs. Y + Nb (b) Nb vs. Y (c) Rb vs. Ta + Yb and (d) Ta vs. Yb [26]. VAG: volcanic-arc granite; Syn-COLG: syn-collision granite; ORG: ocean ridge granite. The field labeled PCG as in Fig. 5d. Symbols as in Fig. 5.

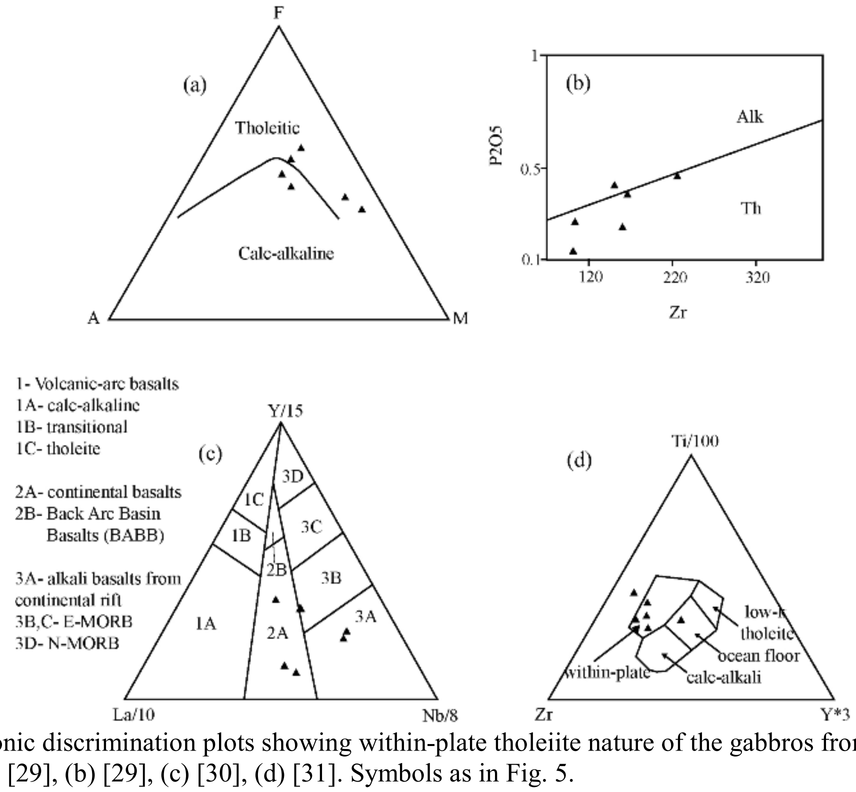

Fig 11. Tectonic discrimination plots showing within-plate tholeiite nature of the gabbros from Ghoshchi area, after (a) [29], (b) [29], (c) [30], (d) [31]. Symbols as in Fig. 5.

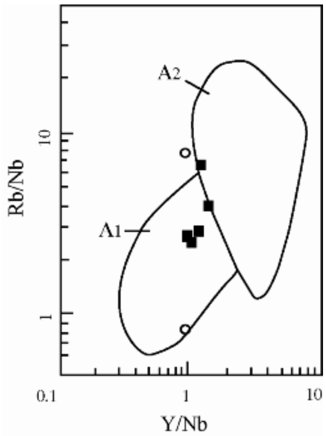

Fig. 12. The A_1 and A_2 subgroup discrimination diagram of A-type granites [32]. Symbols as in Fig. 5.

Petrogenesis

Two main models have been presented for the origin of A-type granites: (1) extensive fractional crystallization of mantle-derived parental mafic magmas [33-34], and (2) partial melting of pre-existing crustal rocks [35-38]. However, the existence of both mantle- and crustal-derived A-type granites has also been advocated [32].

Considerng the coexistence of Mafic and felsic rocks (alkali-feldspar granites) in the studied area, it can be conclude that the petrogenesis of these two types of rocks is connected to each other. However, geochemical evidences indicate obvious differences between biotite granites and alkali-feldspar granites. Biotite granites have crustal source but alkali-feldspar granites have mantle source.

The source of basic rocks in the studied area, is attributed to mantle doming process [15] which caused rifting. Partial melting of upper mantle and generation of basaltic magma and ascend to lower crust, caused melting of crust then generation of granitic magmas.

Gabbro-diorites show a tholeiitic trend. Also, this group have Al_2O_3<17% and quartz and hypersthene in the normative composition, that confirms their tholeiitic character.

Mafic members of Ghoshchi batholith are a suitable source to test the hypothesis of fractional crystallization for the origin of the A-type granites. Modeling of Rayleigh fractionation vectors, which shows the effects of crystallization of a range of selected phase combinations from magmas of different compositions, was performed using the FC-Modeler program of [39]. We have taken the Rb and Y contents of the protolith (Rb= 14 ppm and Y= 17 ppm) from the data on the studied mafic rocks. The vectors show the effect of 85% crystallization of the range of phase combination given in the inset in Fig. 13. Positive trend shown by the plotted alkali-feldspar granites and syenitic rocks supports this idea that the alkali-feldspar granites and syenitic rocks were derived from a parent mafic magma by extensive fractional crystallization (up to ~85%). Contrary, the flat to negative trend displayed by the biotite granites indicates that it should be a separate magma not linked with mafic units through fractional crystallization.

Also, depletion in many elements (Fig. 9) suggests that plagioclase (Ca and Sr) and amphibole (CaO, Fe_2O_3, MgO, TiO_2 and Y) were the dominant fractionating phases during the evolution of the alkali-feldspar granitic magmas. Intense negative Eu anomaly in REE pattern of alkali-feldspar granites (Fig. 9a), confirms the plagioclase fractionation.

Moreover, the P and Ti negative anomalies shown in the multi-element abundances diagram (Fig. 9e) indicate minor fractionation of apatite and Fe-Ti oxide, respectively.

The alkali-feldspar granites show depletion in Al_2O_3, CaO, MgO, Fe_2O_3, TiO_2, P_2O_5, Sr and Ba (Figs. 7 and 8), implying their evolution by extensive fractional crystallization from a less fractionated magma.

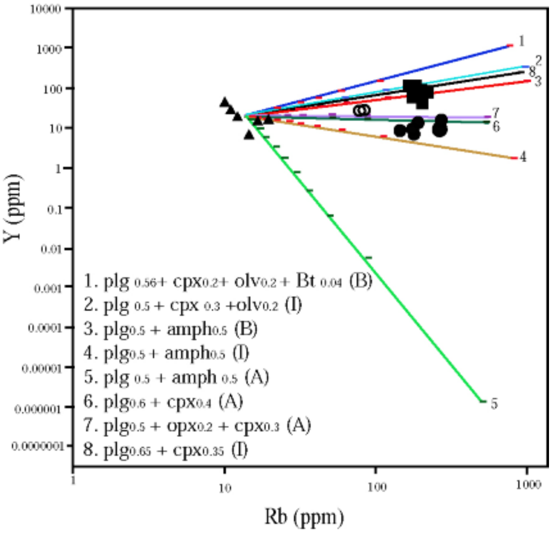

Fig. 13. Y vs. Rb diagram showing Rayleigh fractionation vectors for 85% crystallization. Tick marks along each vector refer to 10% crystallization intervals. Inset shows phase combinations for each vector. A, I, and B = acidic, intermediate and basic melt compositions, respectively. Symbols as in Fig. 5

It has been proposed that A-type granites are originated from the partial melting of LILE-depleted granulitic residue in the lower crust, from which the granitoids melts were previously extracted [35-37]. But the geochemical characteristics of the alkali-feldspar granites, especially their enrichments in LILE (Figs. 9c and e), contradicts sharply with this model.

[16] Believes that A-type granites in NW of Iran are generated due to metasomatism of mafic rocks. The great volume of A-type granite relative to mafic rocks and shortage of petrographic evidence for metasomatism does not confirm this idea. However, there are some evidences that indicate effects of metasomatism in this area in small scale.

Accordingly, we favor the derivation of the Ghoshchi A-type granites from mantle-derived magmas in a post-collision setting with extensive fractional crystallization. Also, the melts are affected by continental crust.

Geodynamic implications

Existence of mafic rocks in the Ghoshchi batholith, suggests the presence of the mantle-derived mafic magmas in the source area of the granites.

The alkali-feldspar granites fall into the A_1 group (mantle derived characteristics) which suggests an anorogenic tectonic setting, but some evidences show that the alkali-feldspar granites are generated in a post-collision extentional regim. Also, gabbro-diorites have within-plate and tholeiitic character. Terefore, it can be conclude that these rocks are generated in an extentional setting.

Deformation in Zagros Basin and opening of Neo-Tethys Ocean commenced during Permian [40-45]. This was a phase of rifting, which flanked the Sanandaj-Sirjan Zone and was associated in the Upper Permian with basic (basalt, diabase, and some intermediate rocks) volcanic activity. There is general agreement that subduction started during the Middle Jurassic, but the time of the continental collision is controversial, Late-Cretaceous [1-2] to Eocene [46-47] or even Miocene [3-48].

It is certain that, the studied granites are formed in an extentional regime eather an anorogenic setting; or a post-orogenic setting. With the available data, it is not possible to distinguish these two, but using field geology data and similar studies in the neighboring area [49], the post-orogenic setting seems reasonable for the studied granites.

If we accept the Cretaceous time for collision, consequently, alkali-feldspar granites will have post-Cretaseous emplacement age.

Accordingly, we favor that the studied alkali-feldspar granites are generated in an extentional regime (post-collision extentions of Neo-Tethys Ocean closure) and then extensive fractional crystallization of mafic tholeiitic rocks.

Biotite granites are generated as a result of partial melting of continental crust due to intruding mafic magmas.

Acknowledgements
This contribution is based on field and laboratory studies carried out at the University of Tabriz. We wish to thank Dr. M. Moazzen for reviewing of manuscript. Also, we thank M. Honarvar and M. Asadpour for sharing their unpublished data and ideas. Thorough and acute comments of two anonymous reviewers have prompted us to re-organise and amend the manuscript.

References
[1] Berberian M., King G.C.P., *"Towards a paleogeography and tectonic evolution of Iran",* Canadian Journal of Earth Science 18 (1981), 210-265.

[2] Mohajjel M., Fergusson C.L., *"Dextral transpression in late Cretaceous continental collision, Sanandaj-Sirjan Zone, western Iran",* Journal of Structural Geology 22 (2000), 1125-1139.

[3] Mohajjel M., Fergusson C. L., Sahandi M.R., *"Cretaceous-Tertiary convergence and continental collision, Sanandaj-Sirjan Zone, western Iran",* Journal of Asian Earth Sciences 21(2003), 397-412.

[4] Ricou L. E., *"Tethys reconstructed: plates, continental fragments and their boundaries since 260 Ma from Central America to south-eastern Asia",* –Geodinamica Acta (Paris) 7 (4) (1994), 169-218.

[5] Şengör A.M.C., *"The Cimmeride orogenic system and tectonics of Eurasia",* Geological Society of America, Special Paper (1984), 195.

[6] Şengör A.M.C., Natal'in B.A., *"Paleotectonics of Asia: fragments of a synthesis"*, In: Yin, A., Harrison, T.M. (Eds.), "The Tectonic Evolution of Asia", Cambridge University Press, Cambridge (1996), 486-640.

[7] Berberian M., Alavi-Tehrani N., *"Structural analysis of Hamadan metamorphic tectonites",* In: Berberian, M., (Eds.), Contribution to the Seismotectonics of Iran (part 3), Geological Survey of Iran, Report 40 (1977), 239-260.

[8] Eftekharnejad J., *"Separation of different parts of Iran based on structural condition in relation to different basins",* Iran Petroleum ints 82 (1981), 19-26.

[9] Jahangiri A., *"Petrology and geochemistry investigation of Goushchi area granites"*, M.Sc. Thesis, Tabriz University, Iran. (1992) (in Persian).

[10] Ghalamghash J., *"Petrology and emplacement of Uromiyeh-Oshnaviyeh plutons",* Ph.D. Thesis, Shahid Beheshti University, Iran. (2002) (in Persian).

[11] Ahmadi Khalaji A., *"Petrology of the granitoid rocks of the Boroujerd area",* Ph.D. Thesis, Tehran University, Iran. (2006) (In Persian).

[12] Agard P., Omrani J., Jolivet L., Mouthereau F., *"Convergence history across Zagros (Iran): Constraints from collisional and earlier deformation"*, International Journal of Earth Sciences 94 (2005), 401-419.

[13] Valizadeh M.V., *"Granites and evolution of the crust in western Iran",* In: Valizadeh, M. V., "Experimental petrology and global tectonic", Vol. 2, "Andesites and Granites",Publ. of Tehran University (1991) 409-423.

[14] Moinvaziri H., *"A preface to magmatism in Iran",* Tarbiat Moallem University, (1996) 440 pp.

[15] Asadpour M., *"Petrology and geochemistry of ultramafic to intermediate rocks of Ghoshchi area",* M.Sc. Thesis, Shahid Beheshti University, Tehran, Iran. (2000) (in persian).

[16] Behnia P., *"Petrogenesis of Ghoshchi area granitoids",* M.Sc. Thesis, Tehran University, Iran. (1995) (in Persian).

[17] Khodabandeh A. A., Amini Fazl A., "*1:100000 Geological map of TASUJ sheet"*, Geol. Survey of Iran. (1993)

[18] Honarvar M., *"Petrogenesis of Ghare Bagh mica ore deposites with a glance to petrology of granites in area",* M.Sc. Thesis, Geol. survey of Iran. (2001) (in Persian).

[19] De La Roche H., Leterrier J., Grand Claude P., Marchal M., *"A classification of volcanic and plutonic rocks using R1-R2 diagrams and major element analyses – its relationships and current nomenclature",* Chemical Geology 29 (1980), 183-210.

[20] Middlemost E.A.K., *"Naming materials in the magma/igneous rock system",* Earth Sciences Reviews 37 (1985), 215-224.

[21] Rickwood P.C., "*Boundary lines within petrologic diagrams which use oxides of major and minor elements"*, Lithos 22 (1989), 247-263.

[22] Küster D., Harms U., *"Post-collisional potassic granitoids from the southern and northern parts of the Late Neoproterozoic east Africa Orogen: a review",* Lithos 45 (1998), 177-195.

[23] Whalen J.B., Currie K.L., Chappell B.W., *"A-type granites: geochemical characteristics, discrimination and petrogenesis"*, Contrib. Mineral. Petrol. 95 (1987), 407-419.

[24] Wu F.Y., Sun D.Y., Li H.M., Jahn B.M., Wilde S., *"A-type granites in northeastern China: age and geochemical constraints on their petrogenesis",* Chemical Geology 187 (2002), 143-173.

[25] Boynton W.V., "*Geochemistry of the rare earth elements: meteorite studies. In: Henderson, P. (ed.), Rare Earth Element Geochemistry*", Elsevier, (1984) 63-114.

[26] Pearce J.A., Harris N.B.W., Tindle A.G., *"Trace element discrimination diagrams for the tectonic interpretation of granitic rocks"*, Geol. Soc. Spec. Publ. 7 (1984), 14-24.

[27] Harris N.B.W., Duyverman H.J., Almond D.C., *"The trace element and isotope geochemistry of the Sabaloka igneous complex. Sudan",* J. Geol. Soc. Lond. 140 (1983), 245-256.

[28] Sun S.S., McDonough W.F., *"Chemical and isotopic systematics of ocean basalts: Implication for mantle composition and processes. In: Saunders, A.D., Norry, M.J., (Eds.), Magmatism in Ocean Basins",* Geological Society of London, Special publication, 42 (1989), 313-345.

[29] Irvine T.N., Baragar W.R.A., *"A guide to the chemical classification of the common volcanic rocks"*, Can. J. Earth Sci. 8 (1971), 523-548.

[30] Winchester J.A., Floyd P. A., *"Geochemical discrimination of different magma seies and their differentiation products using immobile elements",* Chemical Geology 20 (1976), 325-342.

[31] Cabanis B., Leocolle M., *"Le diagramme La/10-Y/15-Nb/8: un outil pour la discrimination des series volcaniques et la mise en evidence des processus de mélange et/ou de contamination crustale",* C. R. Acad. Sci. Paris Sér. II 309 (1989). 2023- 2029.

[32] Pearce J.A., Cann J.R., *"Tectonic setting of basic volcanic rocks determined using trace element analysis",* Earth Planetary Science Letters 19 (1973), 290-300.

[33] Eby G.N., *"Chemical subdivision of the A-type granitoids: petrogenetic and tectonic implicationsv,* Geology 20 (1992), 641-644.

[34] Stern R.J., Gottfred D., *"Petrogenesis of late Precambrian (575-600Ma) bimodal suite in northeast Africa"*, Contributions to Mineralogy and Petrology 92 (1986), 492-501.

[35] Ewart A., Marsh J.S., Milner S.C., Duncan A.R, Kamber B.S., Armstrong R.A., *"Petrology and geochemistry of early Cretaceous bimodal continental flood volcanism of the NW Etendeka, Namibia. Part 2: characteristics and petrogenesis of the high-Ti latite and high-Ti and low_ti voluminous quartz latite eruptions"*, Journal of Petrology 45 (2004), 107-138.

[36] Clemens J. D., Holloway J.R., White A.J.R., *"Origin of an A-type granite: experimental constraints"*, Am. Mineral. 71 (1986), 317-324.

[37] Creaser R. A., Price R.C., Wormald R.J., *"A-type granites revisited: assessment of a residual-source model",* Geology 19 (1991), 163-166.

[38] King P.L., White A.J.R., Chappll B.W., Allen C.M., *"Characterization and origin of aluminous A-type granites from the Lachlan fold belt, southeastern Australia"*, Journal of Petrology 38 (1997a), 371-391.

[39] King E.M., Valley J.W., Turker Barrie C., *"Hydrothermal alteration of oxygen isotope ratios in quartz phenocrysts, Kidd Creek Mine, Ontario: magmatic values are preserved in zircon"*, Geology 25 (1997b), 1079-1082.

[40] Keskin M., *"FC-modeler: a Microsoft Excel spreadsheet programfor modeling Rayleigh fractionation vectors in closed magmatic system",* Computers and Geosciences 28 (2002), 919-928.

[41] Koop W., Stonenly R*., "Subsidence History of Middle East zagros Basin. Permian to recent. Philosophical Transactions of the Royal Society",* London A305pp. (1982) 149-168.

[42] Şengör A.M.C., *"A new model for the Late Paleozoic-Mesozoic tectonic evolution of Iran and implications for Oman",* Geological Society of London, Special Publication 49 (1990), 797-831.

[43] Kazmin V.G., *"Collision and rifting in the Tethys ocean: geodynamic implications",* Tectonophysics 196 (1991). 371-384.

[44] Grabowski Jr., G.J., Norton J.O., *"Tectonic controls on the stratigraphic architecture and hydrocarbon systems of the Arabia plate",* The

Middle East Petroleum Geosciences. (GEOَ) 1 (1994), 413-430.

[45] Stampfli G.M., Marcoux J., Baud A., *"Tethyan margins in space and time"*, Palaeogeography, Palaeoclimatology, Palaeoecology 87 (1991), 373-409.

[46] Stampfli G.M., Mosar J., Faver P., Pillevuit A., Vannay C.J., *"Permo-Mesozoic evolution of the western Tethyan realm: The Neotethys/East Mediterranean connection. Peritethys memoir 6: Peritethyan rift/ wrenchbasins and passive margins"*, International Geological Correlation Program 369 (2001), 51-108.

[47] Numan N.M.S., *"Discussion on "Dextral transpression in Late Cretaceous continental collision, Sanandaj-Sirjan Zone western Iran" "*, Journal of Structural Geology 22 (2001), 8, 1125-1159.

[48] Ghasemi A., Talbot C.J., *"A new tectonic scenario for the Sanandaj-Sirjan zone (Iran) "*, Journal of Asian Earth Science 26 (2006), 683-693.

[49] Agard P., Omrani J., Whitechurch H., Monie P., Jolivet L., *"Zagros geodynamics, from subduction to collision: the fate of the Neotethys"*, Geophysical Research Abstracts, 10 (2008), EGU2008-A-06412.

[50] Mazhari S.A., Bea F., Amini S., Ghalamghash J., Molina J.F., Montero P., Scarrow J.H., *"The Eocene bimodal Piranshahr massif of the Sanandaj-Sirjan Zone, West Iran. A marker of the end of the collision in the Zagros Orogen"*, Journal of Geological Society of London., 166, N.1 (2008), 53-69.

[51] Streckeisen A., *"A chemical approximation to the modal QAPF classification of igneous rocks"*, Neous Jahrb. Mineral. Abh.: (1974) 169-206.

[52] Maniar P.D., Piccoli P.M., *"Tectonic discrimination of granitoids"*, Geo. Soc. Am. Bull. 101 (1989).

[53] Liegeois J.P., Black R., *"Alkaline magmatism subsequent to collision in the Pan-african belt of the Adrar des Iforase"*, In: Fitton, J.G., Upton, B.G.J. (Eds.), "Alkaline Igneous Rocks", 30 (1987). Geological Society, 381-401 (Special Publication).

[54] Shand S.G., *"Eruptive rocks, their genesis, composition, classification and their relation to ore deposits"*, -3rd ed., John Wiley and Sons, (1979) 488 pp.

[55] Chappell B.W., White A.J.R., *"Two constrasting granite types"*, Pac. Geo. 8 (1974), 174-184.

[56] Amiri M., *"Petrographic and petrological study of Almogholagh area minerals (North Asad Abad- Hamedan) "*, M.Sc. Thesis, Tarbiat Moallem University, Tehran, Iran. (1995) (in Persian).

[57] Radfar J., *"Investigation of Astane Arak granite"*. M.Sc. Thesis, Tehran University, Iran. (1987) (in Persian).

[58] Berthier F., Billault J.P., Halbronn B., Maurizot P., *"Etude stratigraphique, Petrologique et structurale de la region de Khorramabad, Zagros, Iran"*, These 3eme cycle, Grenoble, (1974) 282pp.

[59] Shamaniyan Sfahani G. H., *"The study of geochemistry, mineralogy and fluid inclusion in Nezam Abad W mine"*, M.Sc. Thesis, Shiraz University, Iran. (1994) (in Persian).

[60] Soheili M., Jafarian M.B., Abdollahi M.R., *"1:100000 geological map of Aligoodarz sheet"*, Geol. Survey of Iran (1992).

[61] Mohajjel M., Eftekharnejad J., *"1:100000 Geological Map of Golpaygan sheet"*, Geol. Survey of Iran (1992).

[62] Valizadeh M.V., Ghasemi M.R., *"Petrogenesis of Booin-Mian Dasht granitoid"*, Scientific Quarterly Journal of Geosciences 7 (1993), 28-42. (Special Publication).

[63] Valizadeh M.V., Zariyan S., *"Initial petrological investigation on Almoghulagh (Asad abad, Hamedan)"*, Publ. of Faculty of Sciences, Tehran University, 8 (1976). No. 1.

[64] Sepahi Garow A., *"Petrology of Alvand pluton assemblage. Ph.D. Thesis, Tarbiat Moallem University"*, Iran. (1999) (in Persian).

[65] Kholghi M.H., Alavi-Naiini M., *"1:100000 Geological map of Shahin Dezh sheet"*, Geol. Survey of Iran (1994).